Damping models for the sound synthesis of bar-like instruments

Thomas HÉLIE
Analysis-Synthesis Team, Ircam Centre Georges Pompidou, 1 pl. Igor Stravinsky, 75004 Paris, France

and

Denis MATIGNON
ENST/TSI & CNRS, URA 820, 46 rue Barrault, 75 634 Paris Cedex 13, France

ABSTRACT

In this paper, a study on the simulation of damping phenomena in the equation of bars is presented. First, the deflection waves model in a bar for ideal boundary conditions (free bar) is described, and the damping models (fluid damping, stuctural damping) are introduced. Then, a modal analysis allows to discuss the effects of the various parameters of damping and to write the analytical solution of the problem. Finally, numerical simulations are made with the aim of illustrating the various theoretical effects by relevant sound synthesis: physical orders of magnitude are given and a qualitative sound study is made.

Keywords: Sound synthesis, Bars, Damping models, Percussions, Deflection waves.

1 INTRODUCTION

This work is devoted to the sound synthesis of bar-like instruments and refers to [1]; the point of view lies between pure physical modeling (writing down all the governing equations, namely Partial Differential Equations) and signal modeling (typically a Prony model of damped sinusoids). The physical model of a conservative bar (Euler-Bernoulli PDE[1]) is modified by a damping model which introduces extra parameters that do not come from physics. Nevertheless, the damping model is not totally free but pre-structured: it preserves the modal structure of the conservative system, and it is energetically consistent in so far as the hybrid model is now dissipative.

The paper is organized as follows: in § 2 the hybrid model is presented with an emphasis on consistency of the damping model; it is then closely analysed. The role of the two parameters of fluid damping and structural damping respectively is investigated, especially in the spectral domain. Finally, the time-domain signals are presented. In § 3, the parameters are assigned orders of magnitude that are physically consistent; this gives rise to interesting numerical examples followed by a qualitative sound study.

[1] Timoshenko PDE could also be preferred, see [2].

2 PRESENTATION OF THE MODEL

2.1 Equations

In this work, we restrict ourselves to the modeling of the deflection waves of a bar of length L and constant rectangular section $S = w.h$ where w is the width and h the height.

Bars model Let us consider the displacement $\vec{U}(t,x) = u(t,x).\vec{j}$
For an undamped bar, the governing equation of the

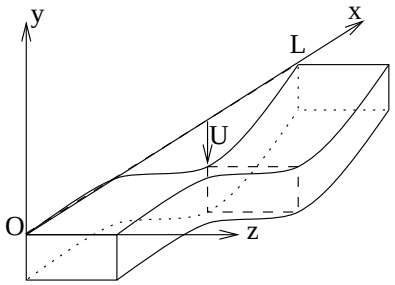

Figure 1: bar model

deflection waves being propagated along (Ox) is written, according to Euler-Bernoulli's theory [3]: for $0 \leq x \leq L$,

$$\frac{1}{\theta^4}.\partial_t^2 u(t,x) + \partial_x^4 u(t,x) \;=\; 0 \qquad (1)$$

where $\theta = \frac{\rho S}{Y I}$ and

$$\begin{cases} \rho & : \text{ density of the material} \\ Y & : \text{ Young's modulus of the material} \\ I = \frac{w h^3}{12} & : \text{ geometrical momentum of the bar} \end{cases}$$

The energy of this bar is given by [4]

$$\mathcal{E}(t) = \frac{1}{2} \int_0^L \left[Y I (\partial_x^2 u)^2 + \rho S (\partial_t u)^2 \right] dx \qquad (2)$$

Moreover, if the bar ends are free and a force of excitation $f_{excit}(t) = -YI\, f(t)$ is applied at $x = 0$, Eq. (9) by the four boundary conditions are expressed by (see [3]):

- no momentum at the ends

$$\partial_x^2 u(t,0) = 0 \qquad (3)$$
$$\partial_x u(t,L) = 0 \qquad (4)$$

- no force at $x = L$ and force $f_{excit}(t)$ at $x = 0$

$$\partial_x^3 u(t,0) = f(t) \qquad (5)$$
$$\partial_x^3 u(t,L) = 0 \qquad (6)$$

Damping models Consider an N-dimensional oscillator of the form $M\,\ddot{x} + K\,x = 0$ with mass matrix $M = M^T > 0$ and stiffness matrix $K = K^T > 0$; it is conservative for the associated mechanical energy $\mathcal{E}(t) = \frac{1}{2}\dot{x}^T M \dot{x} + \frac{1}{2} x^T K\, x$, i.e. $\dot{\mathcal{E}}(t) = 0$. Diagonalizing the system in $\mathbb{R}^N$ leads to the so-called modal decomposition; the scalar dynamics of the n-th component $z_n(t)$ simply reads $m_n\,\ddot{z}_n + k_n\, z_n = 0$ and introduces the natural angular frequencies $\omega_n = \sqrt{k_n/m_n}$.

Such a system is naturally *undamped*. A straightforward way to introduce damping is to add a term involving $\dot{x}$ in the original system: $M\,\ddot{x} + C\,\dot{x} + K\,x = 0$; computing $\dot{\mathcal{E}}(t) = -\dot{x}^T C_s\,\dot{x}$ gives a sufficient condition on C for the new system to be dissipative, namely that C_s, the symmetric part of C, be a *positive* matrix. But if C is not more structured, the modes will be totally changed and the geometry (if not the physics) of the initial problem will be lost. That is the reason why in many applications in vibration, the damping matrix C is *a priori* structured in the following way:

$$C = a\,M + b\,K \qquad (7)$$

This choice has the advantage of preserving the initial modal structure, and of reducing the number of parameters describing the damping from $N(N+1)/2$ down to 2 only. Now, each mode z_n is governed by the damped dynamics $m_n\,\ddot{z}_n + (a\,m_n + b\,k_n)\,\dot{z}_n + k_n\,z_n = 0$, or $\ddot{z}_n + (a + b\,\omega_n^2)\,\dot{z}_n + \omega_n^2\, z_n = 0$, which proves to be dissipative as soon as $a \geq 0$ and $b \geq 0$, more precisely $\dot{\mathcal{E}}(t) = -a\,\dot{x}^T M\,\dot{x} - b\,\dot{x}^T K\,\dot{x} \leq 0$.

This quite simple idea will now be applied to our infinite-dimensional model. Notice that matrices now become operators: the mass operator is $M = 1$ and the stiffness operator is $K = \partial_x^4$. Hence, the following damping operator can be proposed for the Euler-Bernoulli bar:

$$(a + b\,\partial_x^4\ )\,\partial_t \qquad (8)$$

It will preserve the initial modal structure of the conservative system and introduce some dissipativity, though in a rather structured way.

Complete model Thus, the damped bar models are gathered (for various values of the parameters a and b) in the single expression:

$$\frac{1}{\theta^4}\,\partial_t^2 u(t,x) + \left[a + b\,\partial_x^4\ \right]\partial_t u(t,x) + \partial_x^4 u(t,x) = 0 \qquad (9)$$

Hence, Eq. (9) and Eq. (3) to Eq. (6) give the exhaustive description of our system, where $f(t)$ is considered as its input, and $u(x,t)$ its output parametrised by position x.

Positivity constraint Now, the conditions on a and b for which the system is damped (i.e. such as, in free vibrations ($f(t) = 0$), $\frac{d\mathcal{E}}{dt} < 0$) are looked for. Computing $\frac{d\mathcal{E}}{dt}$ from Eq. (2) and then substituting $\partial_t^2 u$ using Eq. (9) leads to:

$$\begin{aligned} \frac{d\mathcal{E}}{dt} &= YI \int_0^L \left[\partial_t \partial_x^2 u\, \partial_x^2 u - a(\partial_t u)^2\right] dx \\ &\quad - YI \int_0^L \partial_t u\, \left[\partial_x^4 u + b \partial_t \partial_x^4 u\right] dx \end{aligned} \qquad (10)$$

Then, a double integration by parts on the second term leads to

$$\begin{aligned} \frac{1}{YI}\frac{d\mathcal{E}}{dt} &= \partial_t u(t,0)\,[f(t) + b f'(t)] \\ &\quad - a \underbrace{\int_0^L (\partial_t u)^2 dx}_{\geq 0} - b \underbrace{\int_0^L (\partial_t \partial_x^2 u)^2 dx}_{\geq 0} \end{aligned} \qquad (11)$$

Hence, in free vibrations, the system is damped when a and b are positive.

2.2 Modal analysis

Resolution of the system in the Laplace domain Let $U(s,x) \triangleq \int_0^\infty u(t,x)\, e^{-st}\, dt = TL[u](s,x)$. Then, Eq. (9) reads (see [3])

$$\Gamma_{a,b}(s)\, U(s,x) + \frac{d^4 U}{dx^4}(s,x) = 0 \qquad (12)$$

where $$\Gamma_{a,b}(s) = \frac{s^2 + a\theta^4 s}{\theta^4 (bs+1)} \qquad (13)$$

Thus, for s fixed, Eq. (12) is a 4th order linear ordinary differential equation whose characteristic equation is

$$k^4 + \Gamma_{a,b}(s) = 0 \quad (14)$$

Then, let k_s be the real positive solution of the four solutions $\{k_s, -k_s, ik_s, -ik_s\}$. Then, the solution of Eq. (12) takes the form

$$U(s,x) = A_s e^{k_s x} + B_s e^{-k_s x} + C_s e^{ik_s x} + D_s e^{-ik_s x} \quad (15)$$

Deriving the expressions of $\partial_x^2 U(s,x)$ and $\partial_x^3 U(s,x)$ from Eq. (15), the four boundary conditions (Eq. (3) to Eq. (6)) can be written $\mathcal{M}_s \,.\, (A_s, B_s, C_s, D_s)^t = F(s)\, k_s^{-3}\, (1,0,0,0)^t$ where $F(s) = TL[f](s)$ and

$$\mathcal{M}_s = \begin{bmatrix} 1 & -1 & -i & i \\ 1 & 1 & -1 & -1 \\ e^{k_s L} & -e^{-k_s L} & -ie^{ik_s L} & ie^{-ik_s L} \\ e^{k_s L} & e^{-k_s L} & -e^{ik_s L} & -ie^{-ik_s L} \end{bmatrix} \quad (16)$$

Finally, A_s, B_s, C_s and D_s are determined, and a filtering relation parametrised by x is obtained:

$$U(s,x) = H(s,x)\,.\,F(s) \quad (17)$$

the transfer function of which is

$$H(s,x) = \frac{N(s,x)}{2k_s^3\,[1-\cosh(k_s L)\cos(k_s L)]} \quad (18)$$

$$\begin{aligned} \text{where } N(s,x) = \; & \sinh(k_s x) - \sin(k_s x) \\ & + \cosh(k_s L)\,\sin\left(k_s(x-L)\right) \\ & - \cos(k_s L)\,\sinh\left(k_s(x-L)\right) \\ & + \sinh(k_s L)\,\cos\left(k_s(x-L)\right) \\ & - \sin(k_s L)\,\cosh\left(k_s(x-L)\right) \end{aligned} \quad (19)$$

Resolution of the system in the time domain From Eq. (17), we find the solution $u(t,x)$

$$u(t,x) = \left[h(.,x) \star f(.)\right](t) \quad (20)$$

where $h(t,x)$ is the inverse Laplace transform of $H(s,x)$.

$H(s,x)$ is a meromorphic function with an infinite countable set of poles $\mathcal{P}$. When both $a, b \geq 0$, this set is located in the left-half complex plane. This will be closely analysed further. For $c > \sup_{s\in\mathcal{P}}\{\Re\mathrm{e}(s)\}$,

$$h(t,x) = \frac{1}{2i\pi}\int_{c-i\infty}^{c+i\infty} H(s,x)\, e^{st}\, ds \quad (21)$$

Finally, using the residue theorem on Eq. (21) leads to the normal-mode expansion

$$h(t,x) = \sum_{s_n\in\mathcal{P}} \operatorname*{res}_{s=s_n}\left\{H(s,x)\right\}.e^{s_n t} \quad (22)$$

in the sense of distributions.

Location of the poles and spectral consequences In order to determine the set of poles, the set $\mathcal{K}$ of the real positive modes $(k_n)_{n\in\mathbb{N}}$ such that $k_n^3\,(1-\cosh(k_n L)\cos(k_n L)) = 0$ is first seeked (cf. Fig. (2)):

$$\mathcal{K} = \left\{0; \frac{4.7300}{L}; \frac{7.8532}{L}; \frac{10.9956}{L}; \frac{14.1372}{L}; \cdots\right\} \quad (23)$$

with $k_0 = 0$ and $k_n \approx \frac{(2n+1)\pi}{2L}$ for n large enough. Then, using Eq. (13) and Eq. (14) gives the two poles associated to each mode.

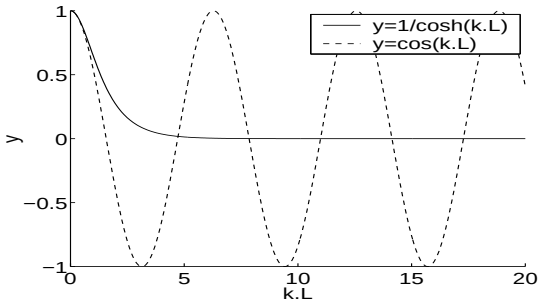

Figure 2: Determination of the modes

Thus, the mode $k_0 = 0$ is associated to the pole 0 which corresponds to the rigid-body motion term, and $s_0 = -\frac{a\theta^4}{2}$ (evanescent wave) which will not be taken into account for sound synthesis purposes. Each mode $k_{n\geq 1}$ is associated to:

$$s_{\pm n} = -\alpha_{\pm n} \pm i\omega_n \qquad (n \geq 1) \quad (24)$$

with $2s_{\pm n} = -\theta^4\left[a + b{k_n}^4\right] \pm \sigma_{a,b}$ and where ${\sigma_{a,b}}^2 = \theta^8[a+b{k_n}^4]^2 - 4\theta^4{k_n}^4$ with the convention $\Im\mathrm{m}(\sigma_{a,b}) \geq 0$. α_n represents the damping coefficient, and ω_n the angular frequency.

Two separate cases appear :

1. When $ab\theta^4 \geq 1$, all modes are evanescent: $\omega_n = 0$ and $\alpha_{\pm n} = \theta^4/2\,\left[a + b{k_n}^4 \mp \sqrt{(a+b{k_n}^4)^2 - 4(k_n/\theta)^4}\right]$.

2. When $ab\theta^4 < 1$, both evanescent and oscillating modes can appear.

For this second case, let K_- and K_+ be the positive numbers defined by ${K_\pm}^2 = (1 \pm \sqrt{1-ab\theta^4})/(b\theta^2)$. Then, the modes k_n are classified as follows:

k_n	0 $\quad K_-$		$K_+ \quad +\infty$
type	evanescent	damped oscillating	evanescent

Now, the locations of the poles for different kind of damping configurations are detailed (note that the orders of magnitude are not physically representative for this theoretical study).

bar without damping In this case ($a = 0$, $b = 0$), $K_- = 0$ and $K_+ = +\infty$). We find $\alpha_{\pm n} = 0$ and $\omega_n = \theta^2 {k_n}^2$.

This corresponds to an everlasting sound for which high modes are quasi-harmonic ($\omega_n{}^2 \propto (2n+1)^2$), Cf. Fig. (3).

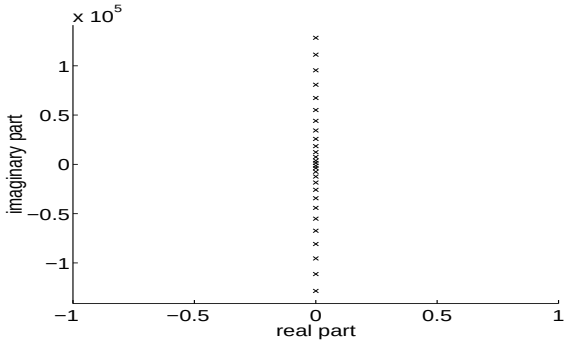

Figure 3: poles for a bar without damping

bar with fluid damping only In this case ($a > 0$, $b = 0$), $K_- = \theta\sqrt{a/2}$ and $K_+ = +\infty$). The first lower modes (a finite number) are evanescent and higher modes are eventually damped oscillating (Cf. Fig. (4)):

- for $k_n \leq K_-$, $\omega_n = 0$ and $\alpha_{\pm n} = \theta^4/2 \left[a \mp \sqrt{a^2 - 4(k_n/\theta)^4}\right]$ *(evanescent).*
- for $k_n > K_-$, $\alpha_{\pm n} = a\,\theta^4/2$ and $\omega_n = \theta^4/2\sqrt{4(k_n/\theta)^4 - a^2}$ *(damped oscillating).*

  The inharmonicity is increased for the first oscillating modes and all of them are uniformly damped since α_n does not depend on n.

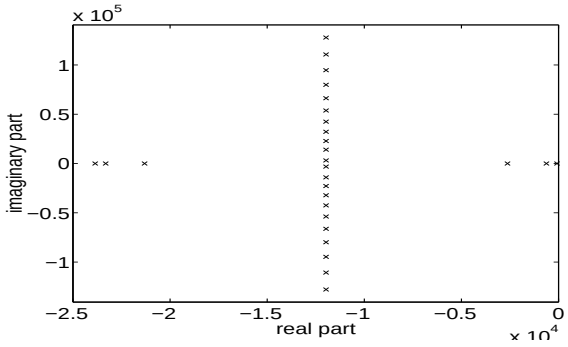

Figure 4: poles for a bar with fluid damping only

bar with structural damping only In this case ($a = 0$, $b > 0$), $K_- = 0$ and $K_+ = \frac{1}{\theta}\sqrt{\frac{2}{b}}$. The first lower modes ($n \neq 0$) are damped oscillating and higher modes are eventually evanescent (Cf. Fig. (5)):

- for $k_n > K_+$, $\alpha_{\pm n} = (\theta k_n)^4/2 \left[b \mp \sqrt{b^2 - 4/(\theta k_n)^4}\right]$ and $\omega_n = 0$ *(fastly evanescent).*

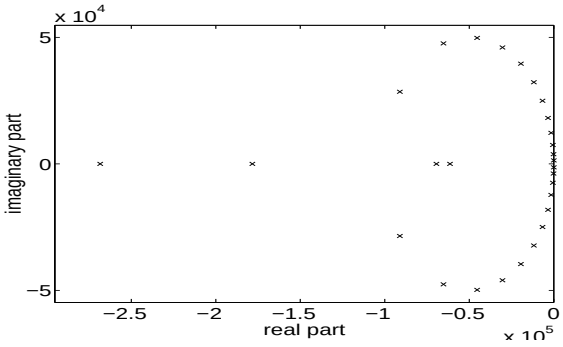

Figure 5: poles for a bar with structural damping only

bar with both dampings In this general case ($a > 0$, $b > 0$ and $ab\theta^4 < 1$), only medium modes are damped oscillating:

- for $k_n \leq K_-$ or $k_n \geq K_+$ $\alpha_{\pm n} = \theta^4/2 \left[a + b{k_n}^4 \mp \sqrt{(a + b{k_n}^4)^2 - 4(k_n/\theta)^4}\right]$ and $\omega_n = 0$ *(evanescent).*
- for $K_- < k_n < K_+$, $\alpha_{\pm n} = \theta^4(a + b{k_n}^4)/2$ and $\omega_n = \theta^4/2\sqrt{4(k_n/\theta)^4 - (a + b{k_n}^4)^2}$ *(oscillating, inharmonic and non uniformly damped).*

From a qualitative point of view, the effects of the fluid damping and of the structural damping appear separately for the first lower modes and the higher modes.

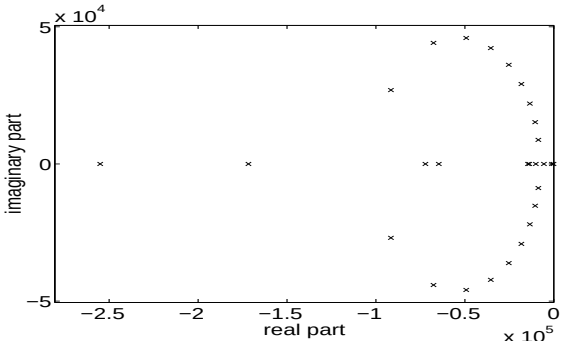

Figure 6: poles for a bar with both dampings

Analytical expression of the impulse responses of the bar displacement and of the acceleration For $n \in \mathbb{Z}^*$, the residues of the simple poles s_n and s_{-n} are computed, and the evanescent component associated to $s_0 = -\frac{a\theta^4}{2}$ is neglected. This enables to give the expression of the impulse response for the displacement $h(t,x)$, and the the impulse response for the acceleration $g(t,x) = \partial_t^2 h(x,t)$ proportional to the force (and hence to the local pressure; a more elaborated model should include a radiation unit, see [5]):

$$h(t,x) = \sum_{n\in\mathbb{Z}^*} h_n\, \phi_n(x)\, \mathrm{e}^{s_n t} \quad (25)$$

$$g(t,x) = \sum_{n\in\mathbb{Z}^*} {s_n}^2 h_n\, \phi_n(x)\, \mathrm{e}^{s_n t} \quad (26)$$

with $h_n = -\left(2\theta^4(bs_n+1)^2\right) / \left(b{s_n}^2 + 2s_n + a\theta^4\right)$, $\phi_n(x) = \lambda_n\,(\sin(k_n x) + \sinh(k_n x)) + \cos(k_n x) + \cosh(k_n x)$ and $\lambda_n = (\cot(k_n L) - \coth(k_n L))^{-1}$.

According to Shannon-Nyquist criterion, only the modes for which the frequency does not go beyond the half sampling frequency are kept in the sum for numerical simulations.

3 NUMERICAL EXAMPLES

In order to build realistic sound examples, sensible physical values are needed to describe the bar. Let's consider:

bar length	: L	=	0.5	m
bar width	: w	=	0.05	m
bar height	: h	=	0.0117	m
Young's modulus	: Y	=	$2.13\ 10^{10}$	Pa
purple wood density	: ρ	=	1015	$kg.m^{-3}$

This gives the modes k_n. For the synthesis, only the first twelve bar modes ($\neq 0$) are taken into account. They are approximatively given by $\{9.46, 15.71, 21.99, 28.27, 34.56, 40.84, 47.12, 53.41, 59.69, 65.97, 72.26, 78.54\}$. When no damping is present, the first and last modes correspond to $f_1 = \omega_1/(2\pi) = 220Hz$ and $f_{12} = 15190Hz$ respectively.

As the damping coefficients are unknown, several physical orders of magnitude are presented: practically, $a \approx 10^{-2}$ and $b \approx 10^{-6}$ seem to be acceptable. Three sounds are synthetised and their respective spectrograms are presented in Fig. (7), Fig. (8) and Fig. (9). Qualitatively, these examples show that b is representative of wooden bar sounds (marimba), whereas a is more representative of metallic bar sounds (xylophone).

It can be heard that both dampings give rise to different audible behaviours and provide a large set of sounds close to percussive bar sounds. These sounds can be downloaded at the following URL: `http://www.ircam.fr/anasyn/helie/barres/sons/`

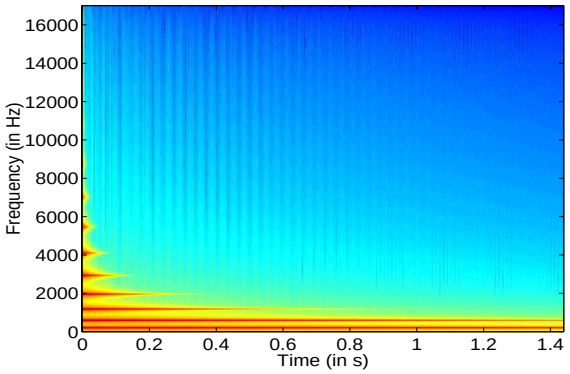

Figure 7: Spectrogram of $g(t,L)$ for $a = 1e-2$ and $b = 5e-7$ (sounds like a wooden bar).

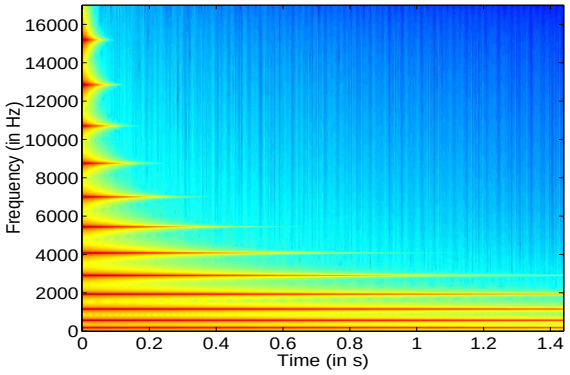

Figure 8: Spectrogram of $g(t,L)$ for $a = 2e-2$ and $b = 5e-8$ (sounds like a glass bar).

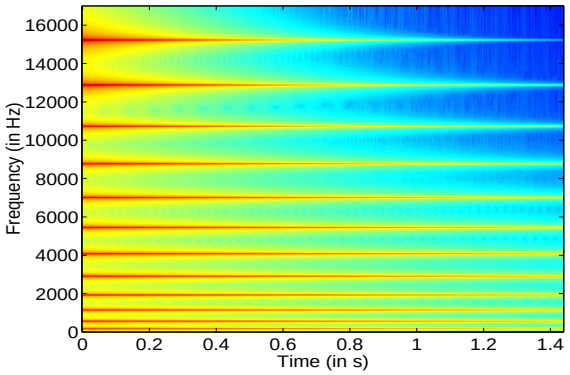

Figure 9: Spectrogram of $g(t,L)$ for $a = 4e-2$ and $b = 3e-9$ (sounds like a metallic bar).

7 CONCLUSION

In this paper, a wide variety of damping models of bar-like instruments has been proposed, closely analysed and numercially simulated; they are energetically consistent and preserve the modal structure of the system; moreover, with the appropriate choice of only two parameters, an infinite number of poles are assigned in the frequency domain, which enables wooden bars, glass-like bars and metallic bars to be synthesized easily, thus proving the usefulness of such hybrid models.

As a straightforward extension, an analogous treatment can be performed on a wave equation, on physical models which are non-uniform in space, and also on even more realistic physical models in 2 or 3 dimensions. Moreover, instead of using the first time derivative as the leading damping term, some non-standard and quite tricky damping models can also be used, which involve fractional derivatives or integrals, and more generally so-called "diffusive representations of pseudo-differential operators" that are dissipative (see [6]); the modal structure is still preserved, but the dynamics of the modes can display some anomalous long-memory behaviour.

REFERENCES

[1] T. Hélie and O. Fidaire. Synthèse sonore et simulation d'amortissements dans l'équation des barres. Master's thesis, École Nationale Supérieure des Télécommunication, Paris, France, june 1997.

[2] A. Chaigne and V. Doutaut. Numerical simulation of xylophones. I. Time-domain modeling of the vibrating bars. *Journal of the Acoustical Society of America*, 101:539–557, 1997.

[3] K. F. Graff. *Wave motion in elastic solids.* Dover publication, New York, 1973.

[4] M. Gérardin and D. Rixen. *Théorie des vibrations.* Masson, Paris, 1993.

[5] V. Doutaut, D. Matignon, and A. Chaigne. Numerical simulation of xylophones. II. Time-domain modeling of the resonator and of the radiated pressure. *Journal of the Acoustical Society of America*, 104(3):1633–1647, September 1998.

[6] D. Matignon, J. Audounet, and G. Montseny. Energy decay for wave equations with damping of fractional order. In *Proc. Fourth international conference on mathematical and numerical aspects of wave propagation phenomena*, pages 638–640, Golden, Colorado, June 1998. Inria-Siam.